Porous hydroxyapatite scafold produced using Musa paradisiaca template and its in vitro bioactivity

by Prihartini Widiyanti

Journal of the Australian Ceramic Society
https://doi.org/10.1007/s41779-021-00677-z

RESEARCH

Porous hydroxyapatite scaffold produced using *Musa paradisiaca* template and its in vitro bioactivity

Ahmad Fadli[1] · Prihartini Widiyanti[2,3] · Deni Noviana[4] · Agung Prabowo[1] · Adi Mulyadi[1] · Deska[1]

Received: 17 August 2021 / Revised: 11 October 2021 / Accepted: 26 October 2021

Abstract
The effect of HA amount on the physical properties and bioactivity of porous HA prepared by replica method using *Musa paradisiaca* as template has been studied. The templates were prepared by cutting the banana fronds into cylindrical shape. Slurries were prepared by mixing 9, 10, and 11 g HA with 11% sago starch, 2.5% Darvan821A, and distilled water. Slurries then stirred at 150 rpm for 24 h. Templates were impregnated into slurry and then dried at 110°C for 2 h. The green bodies were burned at 600°C for 1 h followed by sintering at 1250°C for 1 h. Porous HA was tested in vitro using simulated body fluid solution by soaking for 7–14 days. The cell attachment done by using Baby Hamster Kidney (BHK21) cell. The porous HA was produced with shrinkage in the range of 53.6–58.9%vol, density of 1.26–1.47 g/cm^3, porosity of 53.5–60.1%, and compressive strength of 3.89–4 MPa. The pore size was obtained at the range 71.26–89.13 µm. The biodegradation rate of samples was found at the range of 1.34–2.27% with the increased apatite and carbonate content on porous HA after immersion proven by FTIR result. The cell attachment test showed that the viability of HA was 80.3% confirming that samples were non-toxic material.

Keywords Replica method · Bioceramics · Bioactivity · Simulated body fluid

Introduction

Recently, bone implants manufacture still focuses on the use of metals. Unfortunately, this metals implant is only used for compact bone. This study was conducted in an effort to overcome the need for porous implants. Hydroxyapatite (HA) is the main raw material for scaffolds fabricated. Hydroxyapatite (HA) is an apatite compound which has chemical formula of $Ca_{10}(PO_4)_6(OH)_2$ [1]. HA is a major inorganic component in biological hard tissues such as bones and teeth [2]. HA has excellent biocompatibility, osteoconductivity, and chemical and biological affinity with bone tissue [3]. These properties made HA ideal to be used as component of bones and teeth [4]. In many field of applications, HA is mostly used as porous HA/scaffold HA. Porous HA has high biocompatibility properties and more resorbable compared to HA dense in the form of microcrystals with the size of 190–230 µm from a porous structure that allows blood vessels and connective tissue to enter between the pores to stimulate bone growth. HA scaffold is made to increase the formation of a strong bond between the porous HA and bone. Most research of porous HA shows that the level of tissue infiltration in pores and new bone formation is highly dependent on pore characteristics such as porosity and pore sizes.. The porosity size of HA particles has an important role in the process of bone growth, through the pores of fluid from the connective tissue entering the surface. Certain pore size is favourable to the cytocompatibility just as porosity. Bigger pore size is beneficial for cell attachment and bone formation [5].

The pores in scaffold can be formed by adding pore-forming agents such as starch (sacrificial template method)

✉ Ahmad Fadli
fadliunri@yahoo.com

1 Department of Chemical Engineering, Faculty of Engineering, Universitas Riau, 28293 Pekanbaru, Indonesia

2 Biomedical Engineering-Department of Physics, Faculty of Science and Technology, Universitas Airlangga, 60115 Surabaya, Indonesia

3 Institute of Tropical Disease, Universitas Airlangga, 60115 Surabaya, Indonesia

4 Department of Veterinary Clinic, Reproduction and Pathology, Institut Pertanian Bogor, 16680 Bogor, Indonesia

Published online: 31 December 2021

[5, 6], using air (direct foaming method) [5]; using protein and starch (protein foaming–consolidation method) [7] or by using a template that impregnated by biomaterial suspension (replica/polymeric sponge method) [8]. Replica method/polymeric-sponge method is a method based on the impregnation of cell structures with ceramic suspense to produce macroporous ceramics that have the same morphology as the original porous material [5]. It had open, relatively uniform, and interconnected porous structure on the body [9]. Several materials can be used as templates to fabricate macroporous ceramics using this method. One of that is synthetic porous polymer used by Sopyan and Kaur [8]. In other hand, natural template that has porous structure and well interconnectivity of channel can also be used as template. The use of natural templates is intended to reduce the use of synthetic templates. Natural templates are easier to find and the price is cheaper than synthetic templates and even its used free of charge. Natural templates that can be used must have neat pores and pore structures so that they can adjust to the structure of human pores. In addition, natural templates more easily experience complete combustion at temperatures >600°C so that the resulting porous HA no longer contains impurities. The natural template such as luffa fibers [10] have been used in previous study, luffa fibers were used as pore former agent and nowadays this method uses musa fibers. It is used because it has similar shape with bone in order to achieve better pore structure and interconnectivity than luffa fibers. In addition luffa fibers have larger pore structure than musa fibers so that it was afraid that sample will crack during soaking time and cause data retrieval after the soaking process, prior to use, luffa fibers required several treatment steps so that the use of musa fibers is simpler.

The bioactivity behavior of the porous HA was investigated using in vitro test. In vitro test was done based on modification, by immersing the sample in Simulated Body Fluid (SBF) solution [11]. SBF is a preferred solution model as a simulation of inorganic portions of blood plasma. When blood plasma is at the temperature of 36.5°C, the SBF solution becomes a buffer at pH 7.25; in these circumstances, the concentration of blood plasma ions and SBF closes to the SBF composition. SBF has the same concentration as body fluids [12]. The in vitro test has been done by Swain et al. by using porous scaffold fabricated from polymeric replica sponge method that soaked in SBF solution for 1 week [13]. In our earlier work, we have produced porous HA by using luffa fibers as template according to replica method [10]. The effect of HA solid loading was studied for the physical properties of porous HA. This report presents the effect of HA solid loading on the physical properties and the bioactivity behavior of porous HA during soaking in SBF solution for 2 weeks through replica method. The cell attachment on porous HA was included in this report to evaluate the bioactivity of produced porous HA.

Materials and methods

Materials

Commercial HA powder (Lianyungang Kede Chemical Industry Co. Ltd, China) was used as raw material. Banana fronds (*Musa paradisiaca*) were designated as template which procured from local market in Pekanbaru, Indonesia. The banana fronds (*Musa paradisiaca*) were cut into 1cm in diameter and ± 1.5 cm in height and was dried at room temperature for 1 h. Sago starch (Puri Pangan Sejahtera, Indonesia) was used as binder. Darvan 821A (Vanderbilt Company, USA) was selected as the dispersant agent. Distilled water (Brataco id, Indonesia) was used as solvent.

Preparation of porous HA scaffold

Fabrication of porous HA bodies was preceded by creating a template. The slurry was made by mixing HA, sago starch, distilled water, and Darvan821A by using a magnetic stirrer at a stirring speed of 350 rpm for 24 h, by varying the composition of HA shows on Table 1. The templates (designated banana fronds) were then dipped slowly into the slurry using tweezers so that the slurry enters the pore and covered the templates. Furthermore, templates were dried using an oven at 120°C for 2 h. The combustion process was carried out using a furnace at 600°C for 1 h to remove organic compounds such as banana fronds and binders. The sintering process was carried out at a rate of 3°C/min at temperature of 1250°C for 1 h to produce HA scaffold.

In vitro bioactivity test

In this study, SBF was prepared by mixing 0.8 M KCl ionic solution (0.5 ml), 2 M NaCl (5.6 ml), 0.54 M $NaHCO_3$ (2.78 ml), 0.2 M $MgSO_4.7H_2O$ (0.5 M ml), 52.5 mM $CaCl_2$ (2.5 ml), 0.77M Tris + HCl (5.0 ml), 1.54 M $NaNO_3$ (1.0 mL), and 0.2 M KH_2PO_4 (0.5 ml). The procedure of the preparation of SBF solution follows the Kokubo and Takadama [15]. Final stage that should be achieved for the preparation is pH 7.40 at Temperature 36.5 °C. In vitro test was done

Table 1 Composition of HA, starch, Darvan821A, and distilled water in slurry

Run	HA (gr)	Starch (%)	Darvan821A (%)	Distilled water (ml)
1	9*	11	2.5	35
2	10*	11	2.5	35
3	11*	11	2.5	35

*Based on [14]

based on modification, each sample was weighed to determine the mass of each sample before soaking, then put into 20 mL of SBF solution. SBF solution was taken after 7 and 14 days then filtered using whatman filter paper Number 40. The samples were then dried at 60°C until constant and weighed using analytical scale.

Characterization

The shrinkage was determined by measuring the volume of sample before and after sintering process. The shrinkage was then calculated by using Eq. (1)

$$\%\text{Shrinkage} = \frac{V_b - V_a}{V_b} \quad (1)$$

Vb and Va were sample volumes before and after sintering. The apparent density of sintered porous HA obtained by using Archimedes principles in an Electronic densimeter (Alfa Mirage, MD300S model). The theoretical density of HA 3.16 g/cm^3 was used as reference to calculate total volume of the fraction of porosity. The compressive strength of the porous HA with rectangular shape (10 mm × 10 mm × 10 mm) were measured by Universal Testing Machine (Model 5556 Instron Corp., High Wycombe, UK), at a crosshead speed of 5 mm/min.

Phase analysis was carried out on the porous HA samples after sintering by using *X-ray diffraction* (XRD) analysis using Panalytical XRD XPERT POWDER operating from 10 to 90° 2θ at a step size of 0.026 2θ with CuKa radiation (Kα = 0.15406 nm) at 30 mA and 40 kV. *Scanning electron microscopy* (SEM: Hitachi-SU 3500) was performed to characterize the morphology and microstructure of the sintered porous samples and equipped with an energy dispersive X-ray spectrometer attachment. The average pore size was calculated by using of ImageJ v.151 software. The calcium concentration was measured using *atomic absorption spectroscopy* (AAS) at wavelength 427 nm. Phosphate concentration was measured using UV Spectrophotometer. The functional groups were determined using *Fourier transform infrared spectroscopy* (FTIR). For all sample test used one sample for each variation of HA 9, 10, and 11 g.

In vitro cell attachment on porous HA

Cytotoxicity characterization was successfully carried out using *Baby Hamster Kidney* cells (BHK21). Stages of cytotoxicity testing were initiated by cell culture into 96-*well plate* and incubation with *Dulbecco's Modified Eagle Medium* (DMEM) medium for 22 to 26 h until a partial confluent single layer was formed in the *well* wall. Then the old medium was discarded and replaced with a new 100 mL DMEM medium with placement of sample at *well*. The sample and the new medium were incubated at 37° C for 24 h.

After the incubation, the medium was removed and reagents were added (3-(4,5-*dimethylthiazol*-2-yl)-2,5-*diphenyltetrazolium bromide*) or MTT as much as 20 µL to the *well* and continued the incubation for 4 h. Then, the MTT solution was discarded and the solution was added *Dimethylsulfoxide* (DMSO) as much as 50 µL. *Well* was put into the shaker so that the cells were spread evenly and continued reading the absorbance value with ELISA Reader. This test produced the color intensity of purplish blue formazan products due to cell metabolic activity. The absorbance value was calculated to see cell viability.

Results and discussion

Body properties of porous HA scaffold

Replica method has been used successfully in the fabrication of porous HA by using *Musa paradisiaca* as template. Figure 1 shows porous HA before sintering (b) and after sintering (c). There were burning and sintering processes to produce porous HA after the drying process. Burning step aims to eliminate organic components such as dispersant, sago starch and banana midrib that were contained in green bodies. At burning temperature, the organic components will be completely removed [16]. The sintering process aims to increase the mechanical strength of the material. During the process, porous HA became more compact and the pore

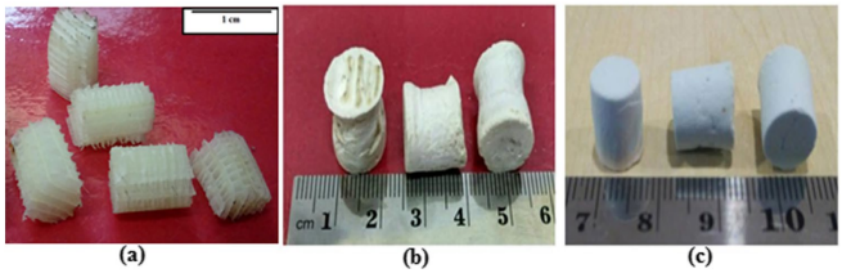

Fig. 1 **a** Templates, porous HA scaffold. **b** Before sintering and **c** after sintering

sizes became smaller during the sintering process thereby increasing the strength of the porous HA scaffold [17].

Figure 1a shows the templates are used in the synthesis process, while Fig. 1b green bodies before sintering with light brown color, and Fig. 1c shows the sintered bodies produced after sintering with light blue color. After the drying process, the resulting green bodies have light brown color. This happened because the organic components are oxidized during the drying process so that color degradation occurred and produced darker color on the green bodies [18]. After the sintering process, the organic component that was lost during the burning process no longer affected the color of the sample so that the color of the sample returned to its original color, i.e., white. It has been reported by Yubao et al. [19] that most commercial HA powders contained small additions of impurities. The origin of the apatite blue color was due to the presence of Mn^{5+} or MnO_4^{3-} ions at the PO_4^{3-} sites in the apatite crystal structure. From the research result, sintering at high temperature not only increases the intensity of oxidation in the oxidizing atmosphere, but also provides enough energy for the oxidized manganese ion (Mn^{2+} to Mn^{5+}) to migrate within the crystal lattice.

Structural feature and mechanical properties

During the sintering process of green bodies, shrinkage occurred. The linear shrinkage of samples at different amount of HA is shown in Fig. 2. By increasing the amount of HA, the shrinkage of sintered porous HA decreased. Shrinkage of the porous HA decreased from 58.9 to 53.6 vol% by varying the amount of HA 9, 10, and 11 g. The increase of amount of HA caused more solids in the slurry. High solids contained in the slurry would reduce shrinkage and prevent the occurrence on the surface of ceramic body [20].

Shrinkage occurred as the organic substances such as dispersant, banana midrib and sago starch were removed. The release of organic substances formed pores in the ceramic body and caused volume shrinkage [21]. Figure 3 shows the density of porous HA as a function of HA amount. It can be seen that the density increased from 1.26 to 1.47 g/cm^3 by varying the amount of HA 9, 10, and 11 g. Total amount of HA in the slurry played important role on the density of porous HA after the sintering process. The total amount of sago starch, dispersant and the shape and structure of templates were kept in same amount by varying the amount of HA, the greater amount of HA in the slurry made the porous HA being denser [20].

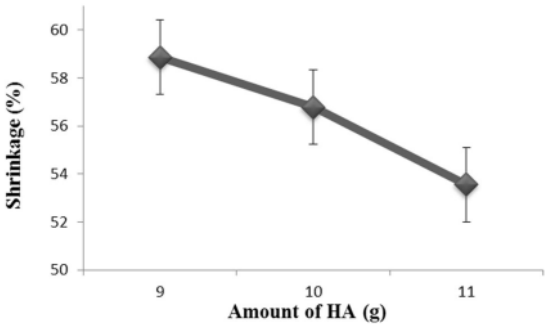

Fig. 2 Shrinkage of porous HA as a function of HA amount

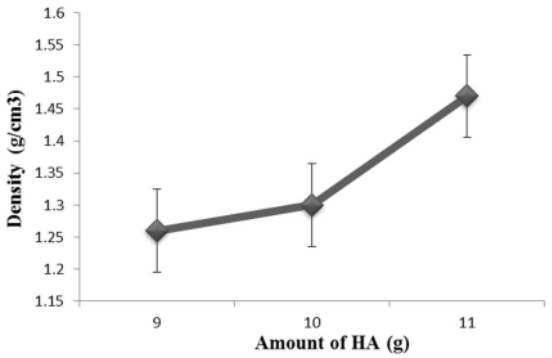

Fig. 3 Density of porous HA as a function of HA amount

Density played important role in determining the microstructure of porous HA. As shown in Fig. 4 and Table 2, it can be seen that a decrease in pore size of porous HA occurred when the density increased. The average pore sizes of porous HA was at the range 71.26–89.13 µm. The more HA contained in the slurry, the smaller size of the pore on sintered porous HA has smaller size after sintering process.

Increasing of HA amount, the density of the sample will increase; it is due to the smaller number of pores formed and causes the mass of the porous body to get heavier, simply as particles that are densification at high temperatures. In the process of sintering the structure of particle material will coarsening and unite to form a unity of mass as densification process. The densification rate will increase if the temperature is higher, the pressure is getting bigger, the particle size is getting smaller and the sintering time is getting longer. The varying in the amount of HA addition of the slurry used also affects the pore size. Pore size get smaller as the density increases. It is because a small percentage caused the number of grains that bind to one another to increase. Bonding the grain interface causes the compressive strength produced from porous scaffolds to increased [22].

Porosity of porous HA increased as the amount of HA increased. The porosity obtained in the range 53.5–60.1%. The highest porosity was found at the addition of 9 g HA which reached 60.1% and the lowest reached 53.481% at the addition of 11 g HA. The addition of HA leads the decrease

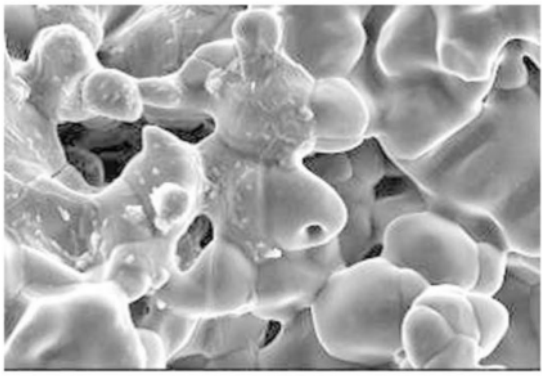

(a)

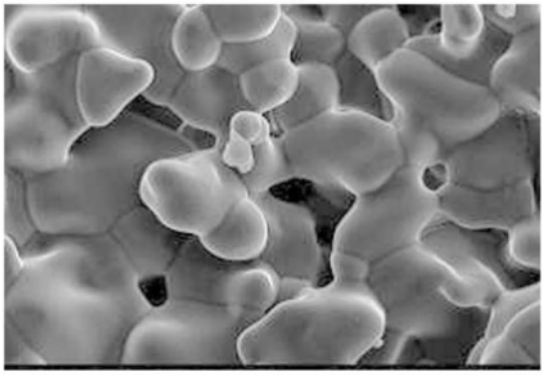

(b)

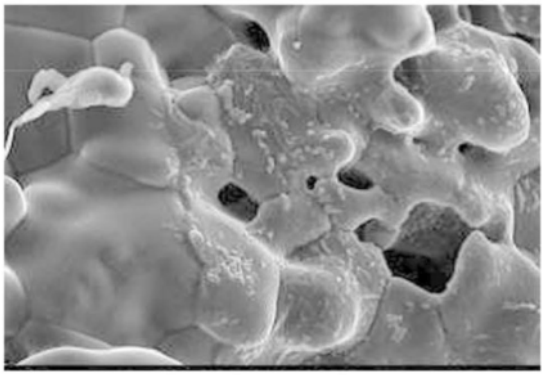

(c)

Fig. 4 SEM micrographs of porous HA with HA amount: **a** 9 g, **b** 10 g, and **c** 11 g

of porous HA porosity as the density increased. The denser porous HA, the less the porous HA and the less decrease of the porosity. Generally, compressive strength of porous HA was strongly affected by the strength of the materials wall (struts) and the surface defects of the strut. The strength of material wall depends on solid loading ceramic [23]. The increase of HA amount leads to the increase of viscosity of

Table 2 The average pore size of porous HA measured at different densities

HA (g)	Density (g/cm^3)	σ (%)	Average pore size (μm)	σ (%)
9	1.26	2.2	89.13	12.8
10	1.30	3.7	79.30	23.5
11	1.47	5.9	71.26	25.7

σ = standard deviations

the slurry [13]. The increased viscosity of the slurry was attributed to the interaction among HA particles, so that the compressive strength of porous HA would be increased and shrinkage would be decreased. The decreased of shrinkage will lead to increases the compressive strength of porous HA due to the sample becomes denser after the sintering process [17]. The compressive strength did not increase significantly, the lower compressive strength in 3.89 MPa in varying of 9 grams HA loading, and higher 4.0 MPa in varying of 11 grams HA loading with the porosity decreases from 60.1 to 53.5% as shown in Fig. 5. A smaller of the porosity caused the number of grains that bind to solidify. The interface of the increasingly dense grain causes the compressive strength of the porous scaffolds to be increased.

Porous HA porosity decreased with the addition of HA due to reduced swelling of starch particles in slurry composition [24]. Gibson and Asby [25] reported that the compressive strength of porous ceramics will increase with decreasing porosity. It can be seen that the porosity affected the compressive strength of porous HA. The XRD (*X-Ray diffraction*) analysis was used to determine the phase and crystal structure of porous HA. The results of XRD analysis data were diffraction peaks that show the phase and compounds that contained in the samples. From Fig. 6, it can be shown that all samples only contain HA. It means that there

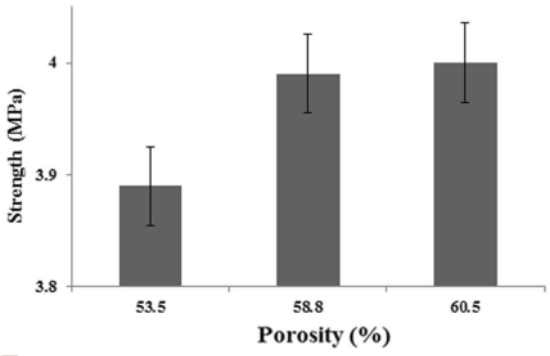

Fig. 5 Compressive strength of porous HA as a function of porosity

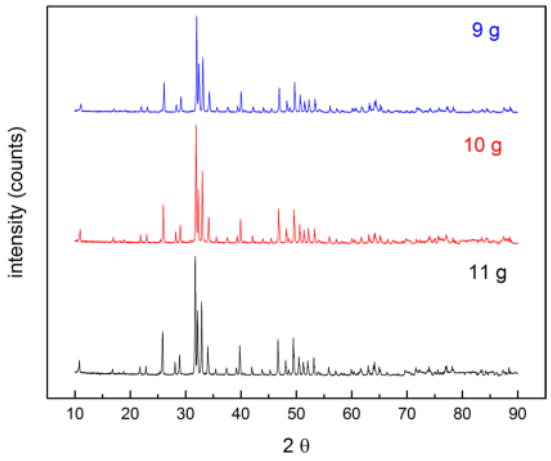

Fig. 6 The XRD patterns of samples with the amount of HA: **a** 9 g, **b** 10 g, and **c** 11 g

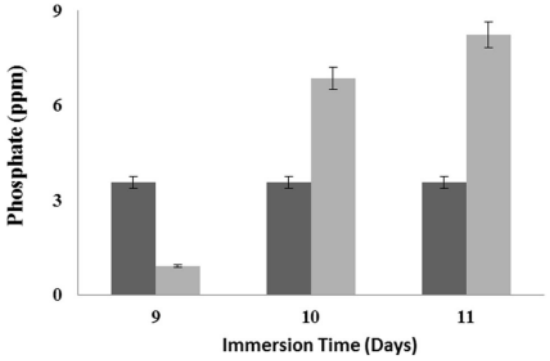

Fig. 7 Changes in phosphate concentration in SBF solution before and after 14 days immersion

were no impurities in the sample after the burning and sintering process. The samples are in crystallite phase proven by the sharp peaks of all samples. The highest peaks were achieved at sample with variation of 11 g HA amount and the lowest were achieved at 9 g HA amount. The increasing of HA amount leads the increase of peaks of samples. The increase of peak height shows that the crystal level of the sample is greater [26].

From the graph above, the resulting porous HA diffractogram have patterns that similar to the pattern of standard HA from the ICDD (*International Centre of Diffraction Data*) data No. 01-072-1243. Samples and standard HA have a hexagonal crystal system proven by the crystalline phase of the samples and standard HA by the sharp peaks. The graph shows that the level of criticism of the sample was the same as the level of crystallinity of the HA standard in the ICDD data.

In vitro bioactivity

Bioresorbtion test was carried out to determine the concentration of calcium (Ca^{2+}) and in the SBF (*simulated body fluid*) solution before and after 14 days immersion. The concentration of calcium in SBF solution before in vitro test was 3.42 ppm and after 14 days of was found – 13.62 ppm. All samples have the same concentration of calcium after 14 days immersion in their own SBF solution. It is clear that the calcium ions decreased significantly after 14 days immersion. The decrease of calcium concentration in the SBF solution was due to the growth of the apatite layer on porous HA [27]. After 14 days of immersion, the precipitation of calcium on the samples resulted in the reduction of calcium in the SBF solution.

The concentration of phosphate was evaluated for the solid phase. Before in vitro test, the phosphate concentration was 3.55 ppm. After 14 days immersion, the phosphate concentration gave different result. For the porous HA with a composition of 9 g HA, the phosphate concentration decreased from 3.55 to 0.9 ppm. Whereas, the porous HA with the composition of 10 and 11 g HA has increased phosphate concentration from 3.55 ppm to 6.85 ppm and 8.24 ppm respectively. From Fig. 7, it can be seen that the highest increasing of phosphate concentration was achieved by porous HA with 11 g HA amount. It showed that porous HA with 11 g HA amount has higher bioactive properties and faster growth of apatite layer compared to porous HA with 9 and 10 g of HA amount.

HA scaffolds after sintering were initially negatively contents on their surface, and joined with positively charged Ca2+ ions in SBF. As a result, amorphous calcium phosphate which is rich in Ca is formed in porous HA. When Ca2+ ions accumulate, porous HA becomes positively charged on its surface and reacts with negatively charged phosphate ions. Thus, amorphous calcium phosphate which has a low Ca level is formed which is then changed to be more stable, namely crystalline apatite such as bone [28].

FTIR (*Fourier transform infrared spectroscopy*) analysis aims to identify the functional groups contained in the samples. The functional groups were identified are OH, CO_3^{2-}, and PO_4^{-3}. The OH^- and PO_{43}^- are the main functional group of HA. The strectching vibrations characteristic of C-O bond was identified as carbonate (CO_3^{2-}) group.

From Fig. 8, it can be seen that the OH^- group with the more intense intensity of %transmittance was found in the porous HA with the composition of HA 9 and 11 g at 3572.32 cm^{-1}. Sample with 10 g HA showed the strongest bond of OH^- group with less

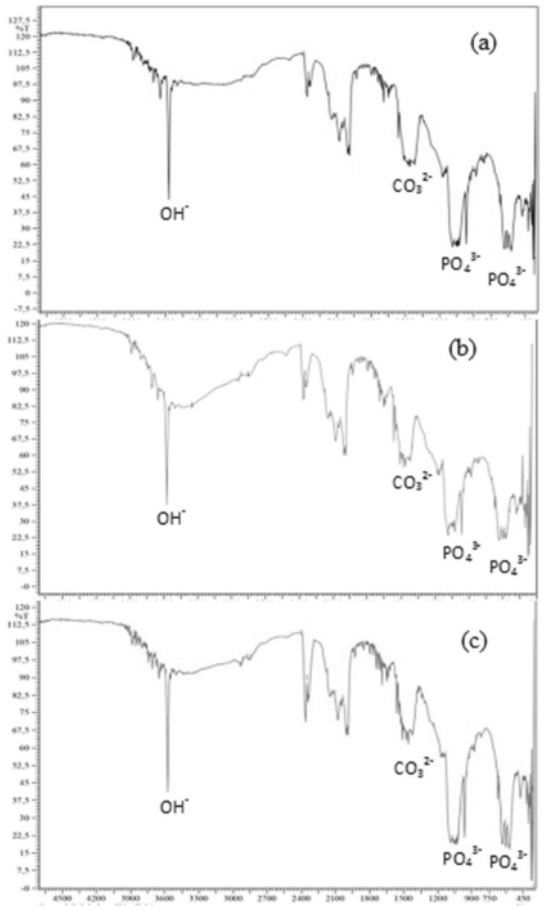

Fig. 8 FTIR analysis after 7 days immersion of HA amount: **a** 9 g, **b** 10 g, and **c** 11 g

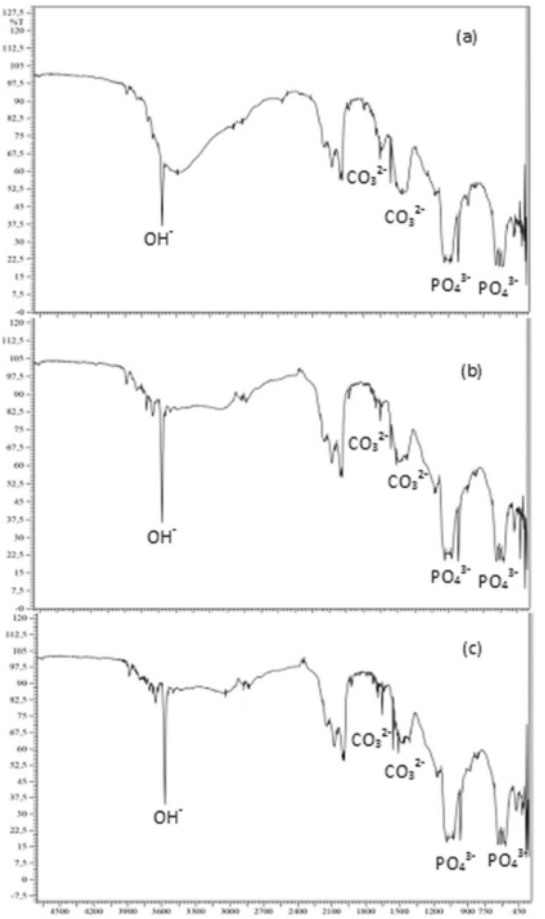

Fig. 9 FTIR analysis after 14 days immersion of HA amount: **a** 9 g, **b** 10 g, and **c** 11 g

%transmittance and shorter wavelength. The C-O bond was found only at sample with HA amount 9 and 10 g at 1464 and 1481 cm^{-1} respectively. The PO_4^{-3} group was found within 1085–600 cm^{-1}. The strongest bond of PO_4^{-3} group was found at sample with HA amount 11g.

The result of FTIR analysis after 14 days of immersion is shown in Fig. 9. The functional OH^- group was found at 3572.32 cm^{-1}, C-O bond at 1412–1653 cm^{-1}, and PO_4^{3-}group at 600–1085 cm^{-1}. The strongest bond of OH^- group was obtained by 9 g HA. The C-O bonds were found more intense than after 7 days of immersion. It means that more carbonate group was identified after 14 days of immersion due to the more precipitation of carbonate on porous HA. The strongest bond of PO_4^{-3} group was found at sample of 11 g HA. This result proven by phosphate concentration that shows the highest increase of phosphate concentration after 14 days of immersion was achieved by sample with 11 g HA (Fig. 7). All samples have less %transmittance of OH^- and PO_4^{3-} groups than samples after 7 days of immersion. It shows that more apatite layers have been produced on porous HA after 14 days of immersion.

The biodegradation test was performed to determine the level of endurance how long porous HA can last before being degraded if it was implanted into human body. Table 3 shows biodegradation during the immersion time in the SBF solution which caused the sample weight decreased. After 7 days of immersion, sample with 11 g HA has the highest mass reduction. This happened because the more HA contained in sample, the faster the release of calcium from sample into SBF solution during the immersion time. It was contrast after 14 days of immersion. Sample with 11 g HA has the lowest mass reduction which was the mass reduction reduced

Table 3 Mass reduction after 7 and 14 days of immersion

HA (g)	Time (days)	Mass reduction (%)	σ (%)
9	7	1.4	0.64
	14	2.27	1.44
10	7	1.45	0.36
	14	1.51	0.49
11	7	1.53	1
	14	1.34	1.21

σ = standard deviations

from 1.53 to 1.3 %mass after 14 days of immersion. In this period, the

phosphate and calcium starts precipitated on porous HA. It was proven by the FTIR result that more phosphate contained in the sample with 11 g HA. Meanwhile, sample with 9 and 10 g HA has increased the mass reduction. The high of biodegradation rate indicates that the precipitation rate from solution to porous HA was lower than the release of calcium from the sample into solution. This biodegradation behavior seems to be a weak point, considering the culture periods of bone tissues [13].

Figure 10 shows the morphology of porous HA at HA amount 9, 10, and 11 g after immersion in the SBF solution for 7 and 14 days.

The results of SEM analysis after in vitro test for 7 days of immersion on porous HA with the amount of HA 9, 10, and 11 g (Fig. 10a, b, and c respectively) showed a change in the growth of apatite crystals on porous HA. Meanwhile, the results after in vitro test for 14 days of immersion showed that there was more apatite crystal growth than 7 days of immersion. This can be seen in Fig. 10d–f for 9, 10, and 11 g of HA amount respectively. The more soaking time for samples in SBF solution, the more apatite layer produced on the surface of each sample [29].

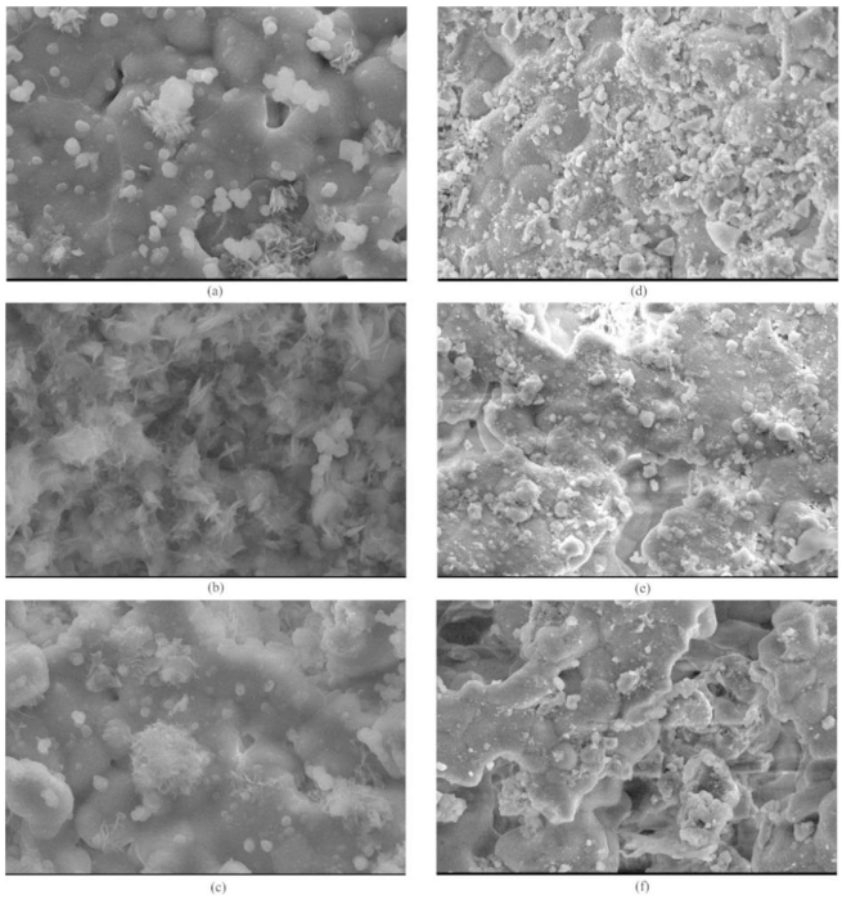

Fig. 10 Microstructure of samples after soaking in SBF solution for **a–c** 7 days and **d–f** 14 days

In vitro cell attachment on porous HA

Based on the results of the cytotoxicity test using the MTT method, HA has a viability value of 80.299%. The results show that the cell viability values were above 70% so that they can be categorized as non-toxic material [30]. This value is in accordance with the theory that HA is the main constituent of bone that has non-toxic properties to the human body [31]. The results show that there are no impurities that cause a decrease in viability. In addition, due to the nature of HA which has many pores, it can facilitate the distribution of cells and nutrients thereby increasing the number of living cells in bone cells [32].

Conclusions

Porous HA have been successfully fabricated by using *Musa paradisiaca* as template. Porous HA was obtained with shrinkage 53.6–58.9%vol, density 1.26–1.47 g/cm^3, porosity 53.5–60.1%, compressive strength 3.89–4.00 MPa, and pore size 71.26–89.13 µm. Variation of HA amount 9, 10, and 11 g does not affect the result significantly. Each sample has a bit different on the result of each other. All samples are accepted as the implant candidates according the physical properties. It was confirmed that *Musa paradisiaca* is able to become a pore former by replica method that gives well result physically

The in vitro test shows that the samples are biocompatible according to their bioresobtion and biodegradation rate results. From FTIR result, it was clear that the longer the immersion time, the more carbonate and apatite precipitated on porous HA. The viability value of 80.299% confirmed that samples are non-toxic material and able to be implanted into human body. The variation of HA amount 9, 10, and 11 g did not affect the in vitro test result significantly as many as the result according to physical properties.

Acknowledgements The authors are grateful for the financial support from Ministry of Research Technology and Higher Education of Indonesia for the financing of this research (no. 21/INS-2/PPKE4/2019).

The authors declare no competing interests.

References

1. Thirumalai, J. Introductory chapter: The testament of hydroxyapatite: new prospect in regenerative medicinal treatments. In *Hydroxyapatite: advances in composite nanomaterials, biomedical applications and its technological facets*; BoD–Books on Demand. 3–14 (2018)
2. Qi, C., Zhu, Y.J., Lu, B.Q., Zhao, X.Y., Zhao, J., Chen, F.: J. Mater. Chem. **2012**(22), 22642–2650 (2012)
3. Zhang, Y., Kong, D., Yokogawa, Y., Feng, X., Tao, Y., Qiu, T.: J. Am. Ceram. Soc. **95**(1), 147–152 (2012)
4. Maheshwari, S.U., Samuel, V.K., Nagiah, N.: Ceram. Int. **40**, 8469–8477 (2014)
5. Studart, A.R., Gonzenbach, U.T., Tervoort, E., Gauckler, L.J.: J. Am. Ceram. Soc. **89**(6), 1771–1789 (2006)
6. Ahmed, Y.M.Z., Ewais, E.M.M., El-Seikh, S.M.J.: Asian Ceram. Soc. **3**, 108–115 (2015)
7. Sopyan, I., Fadli, A., Mel, M.: J. Mech. Behav. Biomed. Mater. **8**, 86–98 (2012)
8. Sopyan, I., Kaur, J.: Ceram. Int. **35**, 3161–3168 (2009)
9. Min, S.-H., Jin, H.-H., Park, H.-Y., Park, I.-M., Park, H.-C., Yoon, S.-Y.: Mater. Sci. For. **2006**(510–511), 754–757 (2006)
10. Fadli, A., Widiyanti, P., Noviana, D., Prabowo, A., Ismawati, H.: J. Rek. Kim. Ling. **15**(2), 62–70 (2020)
11. Sharma, K., Dixit, A., Singh, S., Bhattacharya, S., Prajapat, C.L., Sharma, P.K., Yusuf, S.M., Tyagi, A.K., Kothiyal, G.P.: Mater. Sci. Eng. C **29**(7), 2226–2233 (2009)
12. Kokubo, T., Kushitani, H., Sakka, S., Kitsugi, T., Yamamuro, T.: J. Biomed. Mater. Res. **1990**(24), 721–734 (1990)
13. Swain, S.K., Bhattacharyya, S., Sarkar, D.: Mater. Sci. Eng. C **31**, 1240–1244 (2011)
14. Fadli, A.; Komalasari, K.; Huda, F.; Ardi, T.; Habib, I. J. Nat. Fiber. (2020)https://doi.org/10.1080/15440478.2020.1848698
15. Kokubo, T., Takadama, H.: Biomaterial. **12**(2), 155–163 (2006)
16. Li, S., Huang, B., Chen, Y., Gao, H., Fan, Q., Zhao, J., Su, W.: Int. J. Sur. **11**(6), 477–482 (2013)
17. Kang, S.J.L.: Sintering, densification, grain growth & microstructure. Elsevier Butterworth-Heinemann, Burlington, UK (2005)
18. Kamal, M.M., Baini, R., Mohamaddan, S., Selaman, O.S., Zauzi, N.A., Rahman, M.R., ... Othman, A.K.: Effect of temperature to the properties of sago starch. In IOP Conf. Ser.: Mat, Sci. and Eng. **206**(1), 012–039 (2017)
19. Yubao, L., Klein, C.P.A.T., Xindong, Z., DeGroot, K.: Biomaterials **14**, 969–972 (1993)
20. Fadli, A.; Komalasari. Metode pembuatan komposit berpori menggunakan cara protein foaming-starch consolidation. Indonesia Patent. 2013; P00201304608.
21. Rodríguez-Lorenzo, L.M., Vallet-Regí, M., Ferreira J.M.F.: Fabrication of porous hydroxyapatite bodies by a new direct consolidation method: starch consolidation. J. Biomed. Mater. Res. **60**(2), 232–240 (2002)
22. Kang, S.J.L.: Sintering: densification, grain growth and microstructure. Elsevier. Ch. 4–5, 37–77 (2004)
23. Jamaludin, A.R., Kasim, S.R., Ismail, A.K., Abdullah, M.Z., Ahmad, Z.A.: J. Eur. Ceram. Soc. **35**, 1905–9190 (2015)
24. Garrido, L.B., Albano, M.P., Genova, L.A., Plucknett, K.P.: J. Mater. Res. **13**(1), 39–45 (2008)
25. Gibson, L.J., Ashby, M.F.: Cellular solids structure and properties. Pergamon Press, Oxford (1988)
26. Al-khazraji, K.K., Hanna, W.A., Ahmed, P.S.: Eng. Tech. J. **28**(10), 1880–1892 (2010)
27. Wang, C.X., Zhou, X., Wang, M.: Biomed. Mater. Eng. **14**, 5–11 (2014)
28. Wen, H.B., de Wijin, J.R., Cui, F.Z., de Groot, K.: J. Biomed. Mater. Res. **41**, 227–236 (1998)

29. Takadama, H., Hashimoto, M., Mizuno, M., Kokubo, T.: Round-robin test of SBF for in vitro measurement of apatite-forming ability of synthetic materials. Phosphorus Res Bull. **17**, 119–125 (2004)
30. ISO10993-5. International Standard : Biological evaluation of medical devices-Part 5 Tests for in vitro cytotoxicity (2009)
31. Kantharia, N., Naik, S., Apte, S., Kheur, M., Kheur, S., Kale, B.J.: Dent. Res. Sci Dev. **1**, 15–19 (2014)
32. Murphy, C.M., Haugh, M.G., Brien, F.J.O.: Biomaterials. **31**(3), 461–466 (2010)

Porous hydroxyapatite scafold produced using Musa paradisiaca template and its in vitro bioactivity

ORIGINALITY REPORT

19%	13%	16%	0%
SIMILARITY INDEX	INTERNET SOURCES	PUBLICATIONS	STUDENT PAPERS

PRIMARY SOURCES

1	www.jurnal.unsyiah.ac.id Internet Source	5%
2	Ahmad Fadli, Komalasari, Feblil Huda, Toni Ardi, Ilham Habib. "Optimization of Process Condition on Fabrication of Porous Hydroxyapatite Bodies Using Banana Midrib as Template by Response Surface Methodology", Journal of Natural Fibers, 2020 Publication	2%
3	Ahmad Fadli. "Porous alumina through protein foaming-consolidation method: effect of dispersant concentration on the physical properties", Asia-Pacific Journal of Chemical Engineering, 11/2011 Publication	2%
4	coek.info Internet Source	1%
5	jdream3.com Internet Source	1%

6	www.mdpi.com Internet Source	1 %
7	Zhao, K.. "Porous hydroxyapatite ceramics by ice templating: Freezing characteristics and mechanical properties", Ceramics International, 201103 Publication	1 %
8	media.neliti.com Internet Source	<1 %
9	Charlena, , Irma Herawati Suparto, and Desi Kusuma Putri. "Synthesis of Hydroxyapatite from Rice Fields Snail Shell (Bellamya javanica) through Wet Method and Pore Modification Using Chitosan", Procedia Chemistry, 2015. Publication	<1 %
10	isomase.org Internet Source	<1 %
11	Dobrádi, A., M. Enisz-Bódogh, K. Kovács, and T. Korim. "Bio-degradation of bioactive glass ceramics containing natural calcium phosphates", Ceramics International, 2016. Publication	<1 %
12	worldwidescience.org Internet Source	<1 %
13	ceramics.onlinelibrary.wiley.com Internet Source	<1 %

14	M. Toriyama, A. Ravaglioli, A. Krajewski, G. Celotti, A. Piancastelli. "Synthesis of hydroxyapatite-based powders by mechano-chemical method and their sintering", Journal of the European Ceramic Society, 1996 Publication	<1 %
15	Mardina, Zahrina, N. Fitriana, R. Siswanto, O. Oktavina, N. Zahra, Prihartini Widiyanti, D. Rudyarjo, E. Indarto, and R. Langenati. "The Influence of Braiding Angle Variation in Braided-Twisted Fiber Scaffold Based Poly L-Lactic Acid for Anterior Cruciate Ligament Reconstruction Application", Advanced Materials Research, 2013. Publication	<1 %
16	researcher.life Internet Source	<1 %
17	www.zora.uzh.ch Internet Source	<1 %
18	parasitesandvectors.biomedcentral.com Internet Source	<1 %
19	B Viswanath. "Porous biphasic scaffolds and coatings for biomedical applications via morphology transition of nanorods", Nanotechnology, 11/28/2007 Publication	<1 %

20	Sopyan, I.. "Porous alumina-hydroxyapatite composites through protein foaming-consolidation method", Journal of the Mechanical Behavior of Biomedical Materials, 201204 Publication	<1 %
21	Kim, S.W.. "Fabrication of xenogeneic bone-derived hydroxyapatite thin film by aerosol deposition method", Applied Surface Science, 20081115 Publication	<1 %
22	Masanobu KAMITAKAHARA, Chikara OHTSUKI, Yuko KOZAKA, Shin-ichi OGATA, Masao TANIHARA, Toshiki MIYAZAKI. "Preparation of Porous Glass-Ceramics Containing Whitlockite and Diopside for Bone Repair", Journal of the Ceramic Society of Japan, 2006 Publication	<1 %
23	Yong Huang. "The New Methods and Techniques Based on Gel-Casting", Novel Colloidal Forming of Ceramics, 2010 Publication	<1 %
24	Liang, Lie Feng, Jun Jie Chen, Yong He, and Dai Yang Li. "Preparation and Properties of Porous Hydroxyapatite Ceramics by Three Dimensional Stacking with Homogeneous Fibers", Advanced Materials Research, 2014. Publication	<1 %

25	Takadama, H., and T. Kokubo. "In vitro evaluation of bone bioactivity", Bioceramics and their clinical applications, 2008. Publication	<1 %
26	Xiao, Guiyong, Han Yin, Wenhua Xu, and Yupeng Lu. "Modification and cytocompatibility of biocomposited porous PLLA/HA-microspheres scaffolds", Journal of Biomaterials Science Polymer Edition, 2016. Publication	<1 %
27	discovery.researcher.life Internet Source	<1 %
28	ndl.ethernet.edu.et Internet Source	<1 %
29	www.pertanika.upm.edu.my Internet Source	<1 %
30	core.ac.uk Internet Source	<1 %
31	ethesis.nitrkl.ac.in Internet Source	<1 %
32	virologyj.biomedcentral.com Internet Source	<1 %
33	www.ncbi.nlm.nih.gov Internet Source	<1 %

34	Sopyan, I.. "Preparation and characterization of porous hydroxyapatite through polymeric sponge method", Ceramics International, 200912 Publication	<1 %
35	Xie, Lu, Haiyang Yu, Weizhong Yang, Zhuoli Zhu, and Li Yue. "Preparation, in vitro degradability, cytotoxicity, and in vivo biocompatibility of porous hydroxyapatite whisker-reinforced poly(L-lactide) biocomposite scaffolds", Journal of Biomaterials Science Polymer Edition, 2016. Publication	<1 %
36	Pramanik, S.. "Development of high strength hydroxyapatite by solid-state-sintering process", Ceramics International, 200704 Publication	<1 %
37	Qiang Fu. "Freeze casting of porous hydroxyapatite scaffolds. II. Sintering, microstructure, and mechanical behavior", Journal of Biomedical Materials Research Part B Applied Biomaterials, 08/2008 Publication	<1 %
38	Tae Wan Kim, Su Chak Ryu, Byung Kyu Kim, Seog Young Yoon, Hong Chae Park. "Porous hydroxyapatite scaffolds containing calcium phosphate glass-ceramics processed using a	<1 %

freeze/gel-casting technique", Metals and Materials International, 2014
Publication

Exclude quotes	On	Exclude matches	< 5 words
Exclude bibliography	On		

Porous hydroxyapatite scafold produced using Musa paradisiaca template and its in vitro bioactivity

GRADEMARK REPORT

FINAL GRADE

/0

GENERAL COMMENTS

Instructor

PAGE 1

PAGE 2

PAGE 3

PAGE 4

PAGE 5

PAGE 6

PAGE 7

PAGE 8

PAGE 9

PAGE 10